

## Thermodynamic modeling of phase separation in manganites

J. Sacanell,<sup>1</sup> F. Parisi,<sup>1,2,\*</sup> J. C. P. Campoy,<sup>3</sup> and L. Ghivelder<sup>4</sup>

<sup>1</sup>*Departamento de Física, Comisión Nacional de Energía Atómica, Av. Gral Paz 1499 (1650) San Martín, Buenos Aires, Argentina*

<sup>2</sup>*Escuela de Ciencia y Tecnología, UNSAM, Alem 3901, San Martín, Buenos Aires, Argentina*

<sup>3</sup>*Instituto de Física Gleb Wataghin, UNICAMP, Campinas, SP 13083-970, Brazil*

<sup>4</sup>*Instituto de Física, Universidade Federal do Rio de Janeiro, Caixa Postal 68528, Rio de Janeiro, RJ 21941-972, Brazil*

(Received 9 August 2005; published 5 January 2006)

We present a phenomenological model based on the thermodynamics of the phase separated state of manganites, accounting for its static and dynamic properties. Through calorimetric measurements on  $\text{La}_{0.225}\text{Pr}_{0.4}\text{Ca}_{0.375}\text{MnO}_3$  the low temperature free energies of the coexisting ferromagnetic and charge ordered phases are evaluated. The phase separated state is modeled by free energy densities uniformly spread over the sample volume. The calculations contemplate the out of equilibrium features of the coexisting phase regime, to allow a comparison between magnetic measurements and the predictions of the model. A phase diagram including the static and dynamic properties of the system is constructed, showing the existence of blocked and unblocked regimes which are characteristics of the phase separated state in manganites.

DOI: [10.1103/PhysRevB.73.014403](https://doi.org/10.1103/PhysRevB.73.014403)

PACS number(s): 75.30.Kz, 72.80.Ga

### I. INTRODUCTION

The issue of phase separation is currently one of the main topics of research in strongly correlated electron systems.<sup>1</sup> Phase separation (PS) fully develops in various manganese binary oxides, but there are also evidences of the key role played by clustered states in high  $T_c$  superconductors.<sup>2</sup> Yet, after several years of intense experimental and theoretical research in this area, the true nature of the phase separated state observed in manganites is still controversial. Some phenomenological models points to the strain between the coexisting phases as the main reason for the appearance of phase separated states.<sup>3,4</sup> In addition, there is a lot of theoretical evidence in favor of the role of intrinsic disorder in the stabilization of the phase separated state. These models are based mainly in the double exchange theory, with a fundamental role played by electron-phonon coupling.<sup>5-7</sup> Kagan and co-workers have also pointed out the tendency toward PS of double exchange Hamiltonians when elastic interactions are included.<sup>8</sup>

The presence of quenched disorder can lead to a rough landscape of the free energy densities, triggering the formation of clustered states, which are induced by phase competition.<sup>2</sup> Moreo *et al.* obtained phase separated states in a Monte Carlo simulation of a random-field Ising model when disorder is included in the coupling and exchange interactions.<sup>9</sup> Similar results were obtained by Burgy and coworkers, using a uniform distribution of exchange interactions.<sup>10</sup> As shown for the case of first order transitions, quenched impurities can lead, under certain circumstances, to a spread of local transition temperatures (where local means over length scales of the order of the correlation length) leading to the appearance of a clustered state with the consequent rounding of the first order transition.<sup>11</sup> Typical mechanisms to include disorder are chemical<sup>12</sup> and structural.<sup>13,14</sup>

Despite the intense effort towards a microscopic understanding of the manganites,<sup>15,16</sup> many macroscopic features of the phase separated state, including its thermodynamic

properties and dynamic behavior, still remains to be studied in greater detail. One of the most interesting features of the phase separated state is the entwining between its dynamic and static properties. Some of the phase separated manganites display slow relaxation features that hide experimentally the real equilibrium thermodynamic state of the system.<sup>17</sup> This is why the construction of phase diagrams is currently focused on the dynamic properties of the phase separated state, with regions of the phase diagrams nominated as “frozen” or “dynamic” PS,<sup>18</sup> “strain glass” or “strain liquid,”<sup>19</sup> or, directly, ascribed as spin glass phases.<sup>20,21</sup>

Among the challenging issues which we intend to address is an understanding of the phase separated state in terms of its thermodynamic properties. An analysis of the behavior of phase separated systems based on the probable free energies functional has been schematically realized,<sup>22,23</sup> but without the corresponding measurements supporting the proposed scenario. In the present study we perform an attempt to construct the thermodynamic potentials of the ferromagnetic (FM) and non-FM phases of a PS manganite, through calorimetric and magnetic measurements. The experiments were carried out in a polycrystalline sample of  $\text{La}_{5/8-y}\text{Pr}_y\text{Ca}_{3/8}\text{MnO}_3$  ( $y=0.4$ ), a prototypical phase separated system in which the effects of the substitution of La by Pr produces an overwhelming effect on its physical properties.<sup>12</sup> We took advantage of the fact that in the mentioned compound homogeneous phases can be obtained at low temperatures in longtime metastable states, which allow us to measure separately the specific heat of each phase, CO or FM, in the low temperature region (between 2 K and 60 K). With this data it is possible to write an expression for the difference between the Gibbs energies of the homogeneous phases as a function of temperature and magnetic field. The needed constants to link the thermodynamic potentials of both phases were obtained from indirect measurements based on the static and dynamic behavior of the system. The phase separated state is modeled through the hypothesis that the free energy densities are spread over the sample volume, and

that its nonequilibrium features are governed by a hierarchical cooperative dynamic. Within this framework it is possible to construct a phenomenological expression for the free energy of the phase separated state based on experimental data, which is able to describe consistently the behavior of the system as a function of temperature and applied magnetic field.

## II. EXPERIMENTAL DETAILS

The measurements were made on a polycrystalline sample of  $\text{La}_{0.225}\text{Pr}_{0.4}\text{Ca}_{0.375}\text{MnO}_3$ . Details of material preparation were previously published.<sup>18</sup> Both magnetization and specific heat results were obtained with a Quantum Design PPMS system. Magnetization data was measured with an extraction magnetometer, as a function of temperature, applied magnetic field, and elapsed time. All temperature dependent data was measured with a cooling and warming rate of 0.8 K/min. Specific heat data was measured with a relaxation method, between 2 and 60 K.

## III. RESULTS AND DISCUSSION

Following the  $H$ - $T$  phase diagram of the compound,<sup>18,19</sup> after zero field cooling (ZFC) the sample reaches the low temperature state mainly in the CO phase, a state that has been described as “frozen PS”<sup>18</sup> or “strained glass”<sup>19</sup>. This frozen state can be released by the application of a moderate magnetic field ( $H=2.2$  T),<sup>24</sup> above which the compound transforms into the FM phase in an abrupt metamagnetic transition.<sup>25–27</sup> After this step transition the sample remains in this homogeneous FM state until a temperature around 70 K, even after the magnetic field is removed. These facts were used to perform the measurements of the specific heat  $c^\alpha$  of each phase ( $\alpha=\text{CO}$  or FM) between 2 K and 60 K, each one considered as homogeneous in this temperature range under specific field conditions. In Fig. 1 the plot of  $c/T$  vs  $T^2$  is shown for measurements performed while warming after ZFC with different procedures: under zero field (CO phase), and under different fields  $H$  after a field sweep 0–9 T- $H$ , for  $H=0, 1,$  and 2 T (FM phase). The data of the CO phase and that of the FM are clearly distinguished. Also, the results obtained for the FM phase for the fields employed are practically identical, which is a signature that the FM phase obtained after the application of 9 T remains homogeneous until the highest temperature investigated. Besides, the fact that the specific heats of the FM phase are almost independent of  $H$  is a signal that, in the range of temperature investigated, there is no significant field-dependent contribution to the entropy of the FM phase, indicating that the magnetization is saturated for all fields. The data obtained were adjusted using standard models for CO and FM phases.<sup>28</sup> The small upturn observed at low temperatures corresponds to the onset of the ordering of the magnetic momentum of the Pr atoms.<sup>29</sup>

The thermodynamic Gibbs potential  $g$  of each phase may be written as  $g_0^\alpha(T, H) = E^\alpha(T, H) - TS^\alpha(T, H)$  where the superscript  $\alpha$  indicates the phase (CO or FM), and  $E$  and  $S$  are the enthalpy and the entropy respectively. From the specific

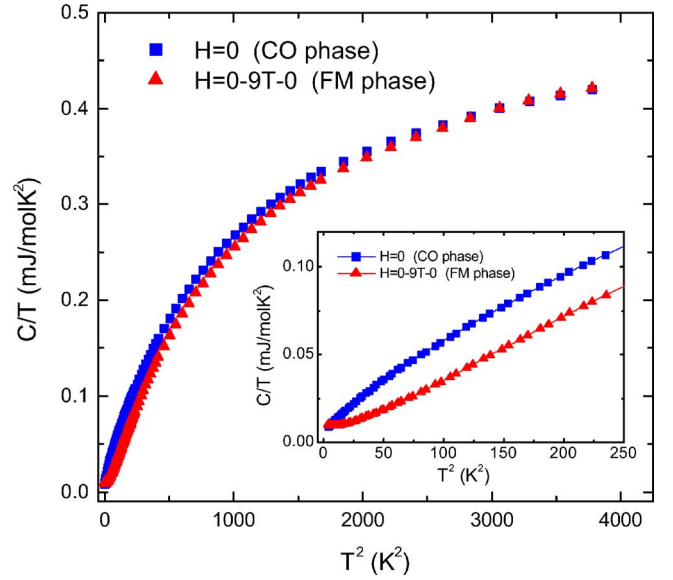


FIG. 1. (Color online) Specific heat of  $\text{La}_{0.225}\text{Pr}_{0.40}\text{Ca}_{0.375}\text{MnO}_3$  as a function of temperature for  $H=0$  in the CO phase (squares) after ZFC, and in the FM phase (triangles) after ZFC to 2 K following of a 0-9 T-0 field sweep. The inset shows an enlargement of the low temperature data.

heat data we could construct both  $E$  and  $S$  in the usual way,<sup>30</sup>

$$E^\alpha(T, H) = E_0^\alpha + \int_{T_0}^T c^\alpha(T) dT - MH, \quad (1)$$

$$S^\alpha(T, H) = S_0^\alpha + \int_{T_0}^T \frac{c^\alpha(T)}{T} dT, \quad (2)$$

where  $M$  is the magnetization of the phase (we assume  $M=0$  for the CO phase) and  $T_0=2$  K is the lowest temperature reached in the measurements. As the specific heat of the FM phase was found almost independent of  $H$ , we consider the Zeeman term in Eq. (1) as the only dependence of the Gibbs potentials of the FM phase with  $H$ , so that  $g_0^{FM}(T, H) = g_0^{FM}(T, 0) - MH$ . No dependence with  $H$  is considered for the CO phase, since there is no way to perform the measurements on the CO phase under an applied  $H$  due to its instability against the application of  $H$  in the temperature upturn. The terms  $E_0^\alpha$  and  $S_0^\alpha$  are respectively the values of the enthalpy and the entropy at the initial temperature  $T_0$ . Since we are interested in the energy difference between the phases involved, we have taken  $E_0^{FM}=0$  and  $S_0^{FM}=0$  as reference values, leaving  $E_0^{CO}$  and  $S_0^{CO}$  as the constant to be determined.

In order to determine  $E_0^{CO}$  we followed the previously published experimental data in relation to the abrupt magnetic transition from the CO to the FM phase, which happens at low temperatures (below 6 K), under a magnetic field of around 2.2 T [ Ref. 24]. This transition is accompanied by a sudden increase of the sample temperature, which reaches a value around 30 K after the transition. Due to the velocity of

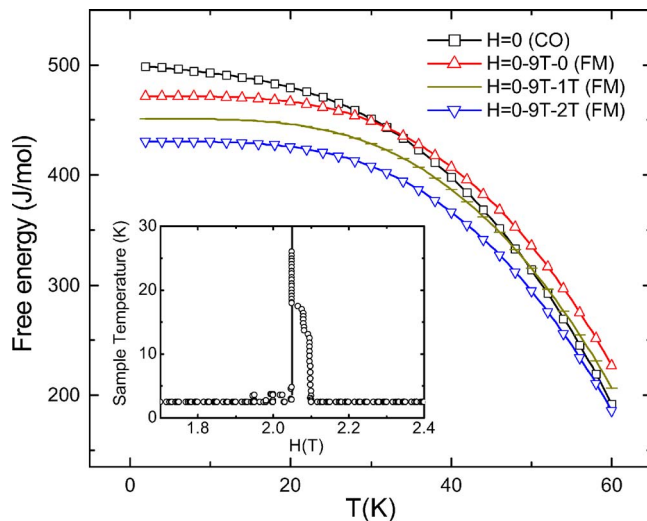


FIG. 2. (Color online) Free energies as a function of  $T$  of the homogeneous phases calculated through Eqs. (1) and (2) for different field sweeps. Inset: temperature of the sample as a function of  $H$  when the step transition occurs (taken from Ref. 18); the base temperature is 2.5 K.

the process, it is plausible to consider that the enthalpy remains constant at the transition point, so that the following relation is fulfilled:

$$E_0^{CO} = \int_{2K}^{30K} c^{FM}(T) dT - M_{sat} H, \quad (3)$$

where  $M_{sat}$  is the magnetization of saturation of the FM phase ( $M_{sat} = 3.67 \mu_B / \text{Mn} = 20.5 \text{ J/mol T}$ ) and  $H = 2.2 \text{ T}$ . This calculation yields  $E_0^{CO} = 28.3 \text{ J/mol}$ , indicating that the homogeneous FM phase has lower free energy at low temperatures even for  $H = 0$ , as suggested in Ref. 18.

In order to fully construct the thermodynamic potentials we have to determine the remaining constant  $S_0^{CO}$  which, at this point, is what controls the transition temperature between the homogeneous phases, providing it is a positive quantity as expected for the difference of entropy between the FM and CO phases due to the excess of configurational entropy of the latter.<sup>22</sup> In Fig. 2 the obtained thermodynamic potentials of the homogeneous phases are displayed, assuming a value  $S_0^{CO} = 0.65 \text{ J/mol K}$ , this value was obtained by adjusting the  $M(H)$  curve of Fig. 4(b), as explained below. The plot indicates that the homogeneous FM state has a lower energy than the CO state for all fields at low temperatures, while the CO phase is the stable state at high temperatures, with field-dependent transition temperatures ranging from 30 K for  $H = 0$  to 60 K for  $H = 2 \text{ T}$ .

The above presented results give us an insight on the behavior of the system under the hypothesis that no phase separation occurs, i.e., describes the thermodynamics of the homogeneous equilibrium phases. In addition, in order to obtain a phase separated state from the thermodynamic data, an appropriate modeling needs to include *a priori* the existence of the phase separated state. However, one needs to be careful when comparing the predictions of the model with

experimental results. It is well established<sup>18,19</sup> that the phase separated state is characterized by a slow dynamics, which implies that equilibrium is hardly reached in laboratory times. The equilibrium properties must be linked with the measured data and therefore a dynamic treatment is needed.

In the discussion that follows we perform a qualitative analysis within a framework where both static and dynamic properties are treated on a phenomenological basis. It is well known that the physical properties of the LPCMO system changes dramatically near  $y = 0.32$ ,<sup>12</sup> revealing the extreme sensitivity of the system to small variations in the mean atomic radius of the perovskite A-site. This can be due to the effects that quenched disorder introduced by chemical substitution has on the local properties,<sup>9</sup> or else to the role played by “martensitic-type” accommodation strains originated by the volume differences between the FM and CO unit cells.<sup>22,13</sup> On one hand, the inclusion of disorder in a random-field Ising model leads to a spatially inhomogeneous transition temperature, from the paramagnetic disordered phase to the “ordered” phase, characterized by the appearance of clustered states.<sup>10,31</sup> This fact implies a spatial dependence of the quadratic coefficient in a Landau-type expansion. On the other hand, strain induced by the shape-constrained transformation between the CO and the FM phases could lead to the phase separated state through the frustration of long-range interactions.<sup>22,13</sup> In the latter view, the properties of a specific compound are governed by an “effective” Pr concentration, which controls the capability of the system to accommodate the anisotropic strain.<sup>22</sup> These two alternative pictures are not mutually exclusive; the clustered states induced by disorder are enhanced if correlated disorder is included in the model,<sup>32</sup> a feature that mimics the cooperative effects of the Jahn-Teller distortion, in a similar way as elastic interactions are able to induce long-scale phase separation in phenomenological models<sup>4</sup> (in this last case, a renormalized fourth order term is responsible for the introduction of spatial inhomogeneities). Additionally, local variations of the atomic composition can couple with the anisotropic strain, triggering the formation of the phase separated state.<sup>22</sup>

These facts can be qualitatively described introducing nonuniform free energy densities for the CO and FM phases. The simplest form is a uniform distribution of these densities over the sample volume, with mean values equal to the free energy of the homogeneous phases. Within the hypothesis that precursor effects of phase separation are due to variations of the local composition, we follow Imry and Wortis’s theory<sup>11</sup> describing the effects of disorder on a system displaying a first order transition in order to estimate the width of the free energies distributions. Following their ideas, and considering that disorder affects mainly the free energy density of the FM phase [ $T_{co}$  is nearly constant as a function of Pr content  $y$  ( Ref. 12)] we can write an expression for the local free energy density  $g^{FM}(\Delta y)$  depending on the fluctuations of composition  $\Delta y$ ,

$$g^{FM}(\Delta y) = g_0^{FM} + (S^{CO} - S^{FM}) \frac{dT_C}{dy} \Delta y, \quad (4)$$

where  $\Delta y$  is taken over length scales comparable with the correlation length, which is around 1 nm for microscopic



clusters in  $\text{Pr}_{0.7}\text{Ca}_{0.3}\text{MnO}_3$ .<sup>33</sup> With the Gaussian distribution proposed in Ref. 11,  $\Delta y$  can be as high as 0.1 over nanometer length scales; the development of micrometer sized domains would need of the consideration of elastic interactions. For the sake of simplicity we take a uniform distribution for  $\Delta y$  over the sample volume. With these assumptions, the free energy density of the FM phase as a function of  $x$  (the volume coordinate is normalized to 1) is written as

$$g^{FM}(x) = g_0^{FM} - \delta(1/2 - x), \quad (5)$$

where  $\delta$  is the parameter controlling the width of the free energy functional, which can be estimated from Eq. (4) as  $\delta \approx (S_{co} - S_{FM})(dT_C/dy)y/2 \approx (70 \text{ K})S_0^{co}$ , taking into account that  $dT_C/dy \approx -350 \text{ K}$  [Ref. 12] and assuming  $\Delta y \approx (y/2)(1/2 - x)$ . In this way, the equilibrium FM fraction  $x_{eq}$  at the given  $T$  and  $H$  is obtained as

$$x_{eq} = \frac{g_0^{CO}(T) - g_0^{FM}(T, H) + \frac{1}{2}\delta}{\delta}. \quad (6)$$

This expression could be used for determining the parameters  $S_{co}$  and  $\delta$ , using, for instance, the  $M(H)$  data at different temperatures. However, as stated before, the global behavior of the system at low temperatures is characterized by out-of-equilibrium features, so the true values for  $x_{eq}$  are not easily accessible experimentally.

In order to circumvent the fact that the thermodynamic equilibrium state is not reached experimentally, an alternative approach is to consider that the response of the system within the phase separated regime as a function of temperature can be qualitatively described within a model of cooperative hierarchical dynamics, using an activated functional form with state-dependent energy barriers.<sup>18</sup> The time evolution of the FM fraction  $x$  is given by

$$\frac{dx}{dt} = \frac{(x_{eq} - x)}{|x_{eq} - x|} \nu_0 e^{-U/(T|x_{eq} - x|)}, \quad (7)$$

where  $\nu_0$  represents a fixed relaxation rate and  $U$  is a (field-dependent) energy barrier scale. This model is similar to that employed to describe vortex dynamics in high  $T_C$  superconductors<sup>34</sup> and is based in dynamic scaling for systems with logarithmic relaxations.<sup>35</sup> The interplay between the dynamic behavior and the equilibrium state of the system is given by the functional form of the effective energy barriers  $U(H)/|x_{eq} - x|$ , which diverge as the system approaches equilibrium. This fact represents the main difference with respect to a pure superparamagnetic behavior, and predicts the existence of state-depending blocking temperatures  $T_B(H, x_B)$  at which, for any given FM fraction  $x_B$ , the system becomes blocked, in the sense that the velocity of change of the FM fraction is lower than, for instance, the detectable velocity  $\nu_{exp}$ , estimated as  $\approx 10^{-6} \text{ s}^{-1}$  for a conventional data measurement that takes 30 s.<sup>18</sup> This gives the following relation for  $T_B(H, x_B)$ :

$$T_B(H, x_B) \leq \frac{U(H)}{|x_{eq} - x_B| \ln(\nu_0/\nu_{exp})}. \quad (8)$$

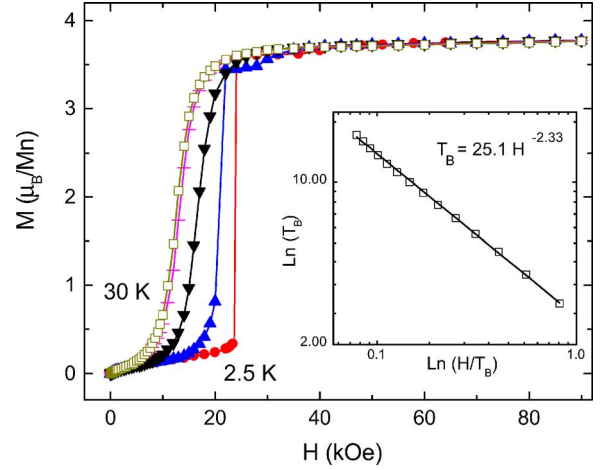


FIG. 3. (Color online)  $M(H)$  data at selected temperatures: 2.5, 8, 15, 25, and 30 K. Inset: log-log plot of  $T_B$  vs  $H/T_B$ , where  $H$  is that for which  $M$  is half of its saturation value.

Through Eq. (8) it is possible to obtain an experimental estimation of the factor  $U(H)/\ln(\nu_0/\nu_{exp})$  which governs the interplay between the dynamics of the system and the measurement procedure. Figure 3 shows  $M(H)$  data for selected temperatures, and the experimentally obtained values of  $T_B(H, x_B = \frac{1}{2})$  as a function of  $H$ , determined through low temperature measurements between 6 and 32 K. The values of  $H$  are those at which the system reaches the state with  $x_B = 0.5$ . The main assumption is that each point of the  $M(H)$  curve corresponds to a blocked state compatible with the measurement procedure. As indicated in the inset of Figure 3, the relation  $\frac{1}{2}T_B(H, \frac{1}{2}) \approx 25H^{-\beta}$  holds, with  $\beta \approx 2.33$ . We will show later that the equilibrium state at low temperatures is fully FM, so Eq. (8) is a direct measurement of the field dependence of the factor  $U(H)/\ln(\nu_0/\nu_{exp}) = \frac{1}{2}T_B(H, \frac{1}{2})$ . Within the dynamic model adopted, this factor is independent of the particular value of  $x_B$  chosen for its determination. With the assumption that this relation holds in the whole temperature range where phase separation occurs, we can write a simple equation relating the equilibrium state with the experimentally accessible state,

$$|x_{eq}(T, H) - x_B(T, H)| \leq \frac{U(H)/\ln(\nu_0/\nu_{exp})}{T}. \quad (9)$$

Through this equation it is possible to make the link between the equilibrium state of the system, which can be obtained through the free energies' functional, and the experimental data obtained through both  $M(H)$  and  $M(T)$  measurements.

The upper panel of Fig. 4 sketches the temperature evolution of  $x_{eq}$  for different magnetic fields, obtained from Eq. (6) with  $S_0^{co} = 0.65 \text{ J/mol K}$  and  $\delta \approx (70 \text{ K})S_0^{co} = 45.5 \text{ J/mol}$ . It shows that, with the set of parameters employed, the low temperature state of the system is fully FM for moderate fields. However, the accessible FM fraction after a ZFC procedure is small for  $H < 2 \text{ T}$ , due to the weight of the blocking term in Eq. (9). This is why, besides the fact that the difference between the free energies of the CO and the FM states increases as temperature is lowered, the magnetic field

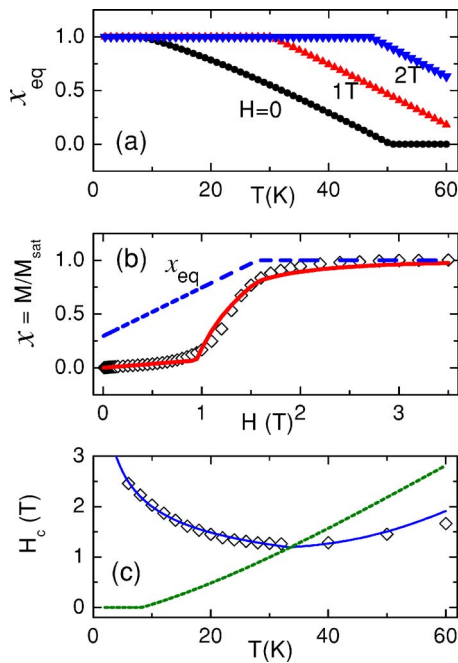


FIG. 4. (Color online) (a) Temperature dependence of the equilibrium FM fraction,  $x_{eq}$ , for the indicated fields. (b) FM fraction  $x$  as a function of  $H$  obtained through  $M(H)$  data (open symbols), and calculated with Eq. (9) (solid line) for  $T=40$  K. The FM equilibrium fraction  $x_{eq}$  obtained from Eq. (6) is also displayed (dashed line). (c) Field needed to make the system half FM, as a function of  $T$ , from  $M(H)$  measurements (open symbols) and calculated through Eq. (9) (solid line). The temperature dependence of the field needed to make the equilibrium state of the system fully FM is also displayed (dashed line).

needed to induce the CO-FM transition also increases, a fact that at first sight could be interpreted as a reentrance of the CO state. As the temperature is raised above 25 K the influence of the blocking term decreases; in this temperature region the main factor determining the field needed to induce the CO-FM transition lies in the field dependence of the equilibrium fraction.

The middle and lower panels of Fig. 4 show the comparison of experimental data with the results obtained through Eq. (9). In Fig. 4(b),  $M(H)$  data at 40 K normalized by its saturation value and the corresponding calculated values are displayed, showing the good agreement between them. Figure 4(c) shows measured and calculated values of the field  $H_c$  at which  $x_B=0.5$ , as a function of temperature; this is the field needed to make half the system FM. Also shown is the temperature dependence of the field needed to make the equilibrium state of the system fully FM. As can be seen, the calculated curve for  $H_c$  reproduces the experimental behavior, with a minimum around 30 K. This minimum signals the crossover from the blocked regime at low temperatures (frozen PS) to the coexistence regime at higher temperatures (dynamic PS). In the frozen PS regime the stable state of the system is homogeneous FM for all fields needed to induce the growth of the FM phase to a value  $x=1/2$ ; the presence of the CO phase is only explained by the slow growing of the FM phase against the unstable CO due to the energy barriers. In the dynamic PS regime, the influence of the blocking term

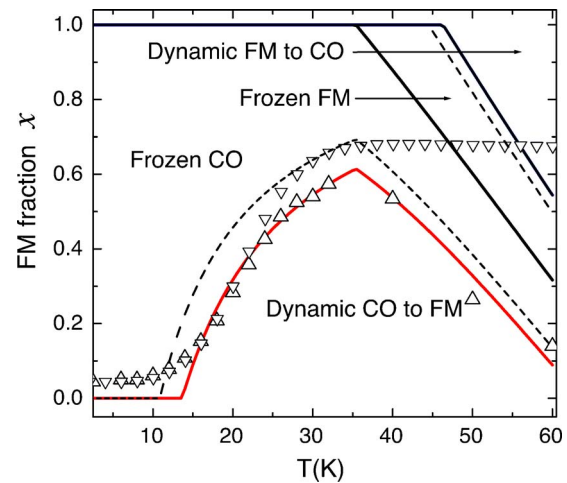


FIG. 5. (Color online) State diagram of the system in the  $x$ - $T$  plane, for  $H=1.3$  T, resulting from Eq. (9). Regions labeled dynamic indicate that the system can evolve in the measured time. Those labeled frozen indicate that the system is blocked. Data obtained from  $M(H)$  measurements at different temperatures (up triangles) and from  $M(T)$  at  $H=1.3$  T after ZFC (down triangles) are also shown. The dashed lines show the new phase diagram boundaries if the measuring time is increased by one order of magnitude.

diminished, the equilibrium state is true PS for moderate fields, and the effect of  $H$  is mainly to unbalance the amount of the coexisting phases.

Figure 5 shows the  $x$ - $T$  state diagram obtained from Eqs. (6) and (9) for a field  $H=1.3$  T, which displays both dynamic and static properties of the model system. A line in the phase diagram divides it in two major regions, depending on the equilibrium FM fraction  $x_{eq}$ . A point above the line indicates that the system has an excess of FM phase; below the line, the state of the system is characterized by the presence of metastable CO regions. Each of these regions is in turn divided in two others, labeled *dynamic CO* or *dynamic FM*, indicating that if the system is in a state within this region is able to evolve toward equilibrium within the measurement time. The regions labeled as *frozen* indicate that the system is blocked, and no evolution is expected within the time window of the experiment. Data points  $x(T, 1.3$  T) obtained from  $M(H)$  and  $M(T)$  measurements are also shown. The  $M(H)$  data is obtained in a field sweep after ZFC to the target temperature, and the  $M(T)$  in a field warming run after ZFC to 2 K. The data extracted from the  $M(H)$  measurements gives information on the  $x$  values for which the system becomes blocked at each temperature, for the specific field and for the characteristic measuring time, indicating the frontier between the dynamic and frozen FM regions. The data obtained from  $M(T)$  measurements coincides with that of  $M(H)$  in the low temperature region, where  $\partial x_B(H, T)/\partial T > 0$ . As the temperature is increased, the system gets into a region for which  $\partial x_B(H, T)/\partial T < 0$  with a FM fraction greater than the lower limit for  $x_B$ , so it remains blocked without changes in the magnetic response, a fact characterized by the plateau observed in  $M(T)$  for the high temperature region. This non-equilibrium phase diagram was constructed for the particular measurement procedure employed for the acquisition of

$M(H)$  and  $M(T)$  data. A modification in this procedure (for instance, by changing the time spent at each measured point) will result in a change in the factor  $\nu_{\text{exp}}$ , with the consequent change of the boundaries in the phase diagram. For example, the effect of increasing the measured time by one order of magnitude is shown by dashed lines in the phase diagram of Fig. 5.

#### IV. CONCLUSIONS

In conclusion, we presented a thermodynamic phenomenological model for a global description of the phase separated state of manganites. The construction starts with the calculation of the free energies of the homogeneous FM and CO phases. The free energies obtained turned out to be very close in value: the difference was of the order of the magnetic energy for intermediate fields in the whole temperature range investigated. The phase separated state is introduced by considering a uniform spread of the free energy density of the FM phase, and the dynamic behavior is included within a scenario in which the evolution of the system is determined through a cooperative hierarchical dynamic with diverging

energy barriers as the system approaches equilibrium. The main success of the model is to provide an understanding of the response of the phase separated state when both temperature and magnetic field are varied, being able to reproduce the dynamic and static properties of the system under study. The same methodology can be also applied to other compounds sharing similar phase diagrams<sup>33,36</sup> and properties, especially those displaying abrupt field-induced transitions at low temperatures.<sup>25–27</sup> The key factor to determine the free energies of the homogeneous phases is the possibility to measure the specific heat of each phase separately, taking advantage of the existence of blocked states, and the measurement of the temperature reached by the compound under study after the CO-FM abrupt transition at low temperature. This last value, and the field at which the abrupt transition occurs, are the key parameters to determine the homogeneous ground state of the system at zero applied field.

#### ACKNOWLEDGMENTS

This work was partially supported by Fundación Antorchas (Argentina) and CAPES, CNPq, and FAPERJ (Brazil).

\*Electronic address: parisi@cnea.gov.ar

<sup>1</sup>E. Dagotto, J. Burgy, and A. Moreo, *Nanoscale Phase Separation in Colossal Magnetoresistance Materials: Lessons for the Cuprates?* (Springer-Verlag, New York, 2002).

<sup>2</sup>G. Alvarez and E. Dagotto, *J. Magn. Magn. Mater.* **272–276**, 15 (2004).

<sup>3</sup>N. D. Mathur and P. B. Littlewood, *Solid State Commun.* **119**, 271 (2001).

<sup>4</sup>K. H. Ahn, T. Lookman, and A. R. Bishop, *Nature (London)* **428**, 401 (2004).

<sup>5</sup>D. I. Khomskii and K. I. Kugel, *Europhys. Lett.* **55**, 208 (2001).

<sup>6</sup>Y. Motome, N. Furukawa, and N. Nagaosa, *Phys. Rev. Lett.* **91**, 167204 (2003).

<sup>7</sup>C. Şen, G. Alvarez, and E. Dagotto, *Phys. Rev. B* **70**, 064428 (2004).

<sup>8</sup>M. Yu. Kagan, D. I. Khomskii, and M. V. Mostovoy, *Eur. Phys. J. B* **12**, 217 (1999).

<sup>9</sup>A. Moreo, M. Mayr, A. Feiguin, S. Yunoki, and E. Dagotto, *Phys. Rev. Lett.* **84**, 5568 (2000).

<sup>10</sup>J. Burgy, M. Mayr, V. Martin-Mayor, A. Moreo, and E. Dagotto, *Phys. Rev. Lett.* **87**, 277202 (2001).

<sup>11</sup>Y. Imry and M. Wortis, *Phys. Rev. B* **19**, 3580 (1979).

<sup>12</sup>M. Uehara, S. Mori, C. H. Chen, and S-W. Cheong, *Nature* **399**, 560 (1999).

<sup>13</sup>V. Podzorov, B. G. Kim, V. Kiryukhin, M. E. Gershenson, and S-W. Cheong, *Phys. Rev. B* **64**, 140406(R) (2001).

<sup>14</sup>P. Levy, F. Parisi, G. Polla, D. Vega, G. Leyva, H. Lanza, R. S. Freitas, and L. Ghivelder, *Phys. Rev. B* **62**, 6437 (2000).

<sup>15</sup>A. Daoud-Aladine, J. Rodríguez-Carvajal, L. Pinsard-Gaudart, M. T. Fernández-Díaz, and A. Revcolevschi, *Phys. Rev. Lett.* **89**, 097205 (2002).

<sup>16</sup>K. J. Thomas, J. P. Hill, S. Grenier, Y-J. Kim, P. Abbamonte, L. Venema, A. Ruydy, Y. Tomioka, Y. Tokura, D. F. McMorro,

G. Sawatzky, and M. van Veenendaal, *Phys. Rev. Lett.* **92**, 237204 (2004).

<sup>17</sup>P. Levy, F. Parisi, L. Granja, E. Indelicato, and G. Polla, *Phys. Rev. Lett.* **89**, 137001 (2002).

<sup>18</sup>L. Ghivelder and F. Parisi, *Phys. Rev. B* **71**, 184425 (2005).

<sup>19</sup>P. A. Sharma, Sung Baek Kim, T. Y. Koo, S. Guha, and S-W. Cheong, *Phys. Rev. B* **71**, 224416 (2005).

<sup>20</sup>F. Rivadulla, M. A. López-Quintela, and J. Rivas, *Phys. Rev. Lett.* **93**, 167206 (2004).

<sup>21</sup>R. Mathieu, D. Akahoshi, A. Asamitsu, Y. Tomioka, and Y. Tokura, *Phys. Rev. Lett.* **93**, 227202 (2004).

<sup>22</sup>M. Uehara and S-W. Cheong, *Europhys. Lett.* **52**, 674 (2000).

<sup>23</sup>N. A. Babushkina, L. M. Belova, D. I. Khomskii, K. I. Kugel, O. Yu. Gorbenko, and A. R. Kaul, *Phys. Rev. B* **59**, 6994 (1999).

<sup>24</sup>L. Ghivelder, R. S. Freitas, M. G. das Virgens, M. A. Continentino, H. Martinho, L. Granja, M. Quintero, G. Leyva, P. Levy, and F. Parisi, *Phys. Rev. B* **69**, 214414 (2004).

<sup>25</sup>R. Mahendiran, A. Maignan, S. Hébert, C. Martin, M. Hervieu, B. Raveau, J. F. Mitchell, and P. Schiffer, *Phys. Rev. Lett.* **89**, 286602 (2002).

<sup>26</sup>L. M. Fisher, A. V. Kalinov, I. F. Voloshin, N. A. Babushkina, D. I. Khomskii, Y. Zhang, and T. T. M. Palstra, *Phys. Rev. B* **70**, 212411 (2004).

<sup>27</sup>D. S. Rana, R. Nirmala, and S. K. Malik, *Europhys. Lett.* **70**, 376 (2005).

<sup>28</sup>V. Hardy, A. Maignan, S. Hébert, and C. Martin, *Phys. Rev. B* **67**, 024401 (2003).

<sup>29</sup>V. N. Smolyaninova, A. Biswas, X. Zhang, K. H. Kim, B. G. Kim, S-W Cheong, and R. L. Greene, *Phys. Rev. B* **62**, R6093 (2000).

<sup>30</sup>L. D. Landau and E. M. Lifshitz, *Statistical Physics* (Butterworth-Heinemann, Oxford, 1999).

<sup>31</sup>H. Aliaga, D. Magnoux, A. Moreo, D. Poilblanc, S. Yunoki, and

- E. Dagotto, Phys. Rev. B **68**, 104405 (2003).
- <sup>32</sup>J. Burgy, A. Moreo, and E. Dagotto, Phys. Rev. Lett. **92**, 097202 (2004).
- <sup>33</sup>P. G. Radaelli, R. M. Ibberson, D. N. Argyriou, H. Casalta, K. H. Andersen, S.-W. Cheong, and J. F. Mitchell, Phys. Rev. B **63**, 172419 (2001).
- <sup>34</sup>G. Blatter, M. V. Feigel'man, V. B. Geshkenbein, A. I. Larkin, and V. M. Vinokur, Rev. Mod. Phys. **66**, 1125 (1994).
- <sup>35</sup>A. Labarta, O. Iglesias, Ll. Balcells, and F. Badia, Phys. Rev. B **48**, 10240 (1993).
- <sup>36</sup>J. Hejtmánek, Z. Jiráček, J. Sebek, A. Strejček, and M. Hervieu, J. Appl. Phys. **89**, 7413 (2001).